Lactide-caprolactone copolymers with tuneable barrier properties for packaging applications

Ainara Sangroniz*[1], Leire Sangroniz[1], Shaghayegh Hamzehlou[2], Javier del Río[3], Antxon Santamaria[1], Jose Ramon Sarasua[4], Marian Iriarte[1], Jose Ramon Leiza[2], Agustin Etxeberria*[1]

[1]POLYMAT, Department of Polymer Science and Technology, Faculty of Chemistry, University of the Basque Country UPV/EHU, Manuel de Lardizabal 3 Pasealekua, Donostia 20018, Spain.

[2]POLYMAT, Department of Applied Chemistry, Faculty of Chemistry, University of the Basque Country UPV/EHU, Joxe Mari Korta Zentroa, Tolosa Hiribidea 72, Donostia 20018, Spain.

[3]Department of Material Physics, Complutense University of Madrid, Ciudad Universitaria s/n, Madrid 28040, Spain.

[4]POLYMAT, Department of Mining-Metallurgy Engineering and Materials Science, University of the Basque Country UPV/EHU, Torres Quevedo Ingeniariaren Plaza 1, Bilbo 48013, Spain.

* Correspondence to:

Ainara Sangroniz (E-mail: ainara.sangroniz@ehu.es)

Agustin Etxeberria (E-mail: agustin.etxeberria@ehu.es)

Abstract

Lactide-caprolactone copolymers have been synthetized employing two metallic catalysts, Ph_3Bi and $SnOct_2$. The analysis of the microstructure by NMR reveals that gradient like copolymers are obtained with $SnOct_2$ catalyst, whereas for Ph_3Bi based copolymers the gradient like character is less pronounced. The incorporation of caprolactone reduces the crystallinity degree and the glass transition temperature, leading to a slight increase of the free volume fraction. Thermal properties, free volume fraction and chemical nature of the penetrant are correlated with obtained oxygen and water vapour permeability. It is demonstrated that selecting adequate compositions of lactide-caprolactone copolymers it is possible to broaden the field of biodegradable polymers in packaging applications.

Keywords

Polylactide, packaging, permeability

1. Introduction

Plastic production has increased from 15 MT in 1964 to 348 MT in 2017 and it is expected that it will continue increasing in the next years. According to the European plastics converter demand, packaging is the most important sector (39.9 %), followed by building and construction and automotive industry [1]. In fact, polymers are the most widely employed materials in packaging applications due to their low cost, great performance and easy processability. Furthermore, plastics contribute to the reduction of the fuel consumption in transportation by bringing down the weight of the packaging.

Nowadays, the most employed materials in packaging are polyolefins and poly(ethylene terephthalate), which show a good barrier character to gases and vapours and good mechanical performance [1]. However, after a short period of use, they are disposed contributing to the huge problem of plastic waste. Currently the three main methods for the disposal of plastic waste are burying them in the landfills, mechanical recycling, where the properties of the material are deteriorated, and energy recovering [1]. An alternative solution to this problem is the use of biodegradable polymers that under adequate conditions can be degraded into carbon dioxide, biomass and similar substances. Therefore, no waste is generated contributing to the circular economy.

Poly(lactide) has gained considerable interest among biodegradable polymers, because it is biocompatible and can be obtained from renewable resources. These features, besides thermoplastic like processability and high thermal stability makes this material suitable for food packaging. However, its poor mechanical performance in regard to ductility can make it not the most appropiate for this application [2,3].

In order to improve its properties different strategies have been identified. One of them is the synthesis of copolymers choosing comonomers such as ε-caprolactone and other macrolactones leading to copolymers behaving ductile or elastomer thermoplastic [4]. In this sense, the copolymerization strategy allows also to combine the properties of each homopolymer including the barrier properties [5-6]. Changing the lactide-caprolactone composition, chain microstructure and multiblock sequence length distributions [7,8] it is possible to obtain a range of properties from rigid plastic to elastomeric to obtain materials *ad hoc* to each application [9]. In literature the synthesis of lactide-caprolactone copolymers has been widely studied and great efforts have been done to obtain truly random copolymers [10-12]. Considering the potential application

of lactide based copolymers, containing caprolactone as well as other macrolactones copolymers, as potential biomaterials for controlled drug release, templates for tissue engineering and medical implants, their mechanical properties and biodegradation studies have been a previous subject of interest [7,8]. However, there are not extensive works analysing the physical properties of those copolymers, notwithstanding this is of paramount importance to ascertain the suitability of these materials for packaging applications.

In this work, lactide/caprolactone copolymers have been synthetized by ring opening polymerization employing two catalysts: stannous octoate ($SnOct_2$) and triphenyl bismuth (Ph_3Bi). The first one has been approved by the US FDA as food additive [13]. Regarding the later, it has been proved that bismuth is less toxic than zinc and some bismuth compounds are used as drugs for different affections [13]. Copolymers of different compositions have been synthetized and the kinetics of the copolymerization and the chain microstructures of the copolymers during the reaction have been analysed with both catalysts. The most adequate copolymers have been selected *a priori* and their thermal properties, free volume fraction and permeability have been studied to analyse the suitability of lactide-caprolactone copolymers for packaging applications.

2. Experimental part

2.1. Materials and synthesis procedure

Materials and methods

Air and moisture sensitive materials were synthetized and manipulated in an inert gas filled glovebox or on a high vacuum line. L-lactide was purchased from Futerro and it was recrystallized from dried toluene prior to utilization. ε-caprolactone was purchased from Sigma Aldrich and it was distilled before utilization. Stannous octoate and triphenyl bismuth were purchased from Sigma Aldrich and Gelest, respectively, and they were used as received.

Synthesis of copolymers

The general procedure for the reaction is described below. The copolymerizations for the kinetic analysis were performed at 150 °C and 500:1 monomer:catalyst ratio for 5 hours. The reactions were carried out in 0.5 g scale in small glass vials. At adequate times aliquots were withdrawn and analysed by ^{1}H NMR.

The polymerization and copolymerization large scale reactions (10 g) were carried out at 150 °C for 4 hours and at 500:1 monomer:catalyst ratio, following a similar procedure reported by Fernández et al. [8,14,15]. The reaction was performed in a glass reactor (size 250 mL) with mechanical stirring. The obtained polymers were purified by dissolving in chloroform and precipitating in cold methanol. Afterwards, the materials were dried at 70 °C for 48 h.

Preparation of samples

Films of 50–100 μm thick were prepared by casting using chloroform as solvent (5 % polymer weight concentration). The solution was poured into a petri dish and after 24 h at room temperature it was dried in an oven at 70 °C for 5 days under vacuum and 2 more days at room temperature, also under vacuum.

1 mm thick sheets for rheological and free volume measurements were prepared by compression moulding at 190 °C and 100 bar.

2.2 Experimental techniques

NMR spectra

Proton and carbon nuclear spectra were recorded on a Bruker Avance DPX 300 spectrometer at 300.16 MHz and 75.5 MHz resonance frequency, respectively, employing 5 mm internal diameter tubes and at room temperature (30 °C). For ^{1}H NMR results, 10 mg of sample were dissolved in 0.4 mL deuterated chloroform and 32 scans were performed. In the case of ^{13}C NMR 40 mg of sample were dissolved in 0.4 mL of deuterated chloroform and more than 5000 scans were performed.

Molar mass

The molar mass of the samples was determined employing size exclusion chromatography (SEC, Thermo Scientific) using a Waters 717 autosampler with a differential refractometer (Waters 2410), a pump (Dionex Ultimate 3000), a refractive index detector (RI, Refracg-to Max 521) and four Phenogel GPC columns (Phnenomenex) with 5 μm particle size and 10^5, 10^3, 100 and 50 Å porosities. The measurements were performed in tetrahydrofuran at a flow rate of 1 mL min^{-1} and 30 °C. The molar masses were referred to poly(styrene) standards.

In the case of the measurements performed in chloroform another equipment was employed: Waters 1515 GPC device with two Styragel columns (10^2-10^4 Å). The flow

of the eluent was 1 mL min^{-1} and the molar masses were referred to poly(styrene) standards.

Thermal analysis

Thermal properties were determined by a differential scanning calorimeter (DSC) from TA Instruments, model Q2000 V24. Samples of approximately 5 mg were encapsulated in aluminium pans. First a scan from -80 to 200 °C at a heating rate of 10 °C min^{-1} was carried out to determine the thermal properties of the films. Then, the sample was cooled down to -80 °C at 10 °C min^{-1} and heated again up to 200 °C at the same rate to determine the glass transition temperature.

The crystallinity degree of the samples was calculated using the following equation:

$$X_c = \frac{\Delta H_m}{\Delta H_m^0} \times 100 \quad (1)$$

where ΔH_m is the experimental value of the melting enthalpy and ΔH_m^0 is the theoretical value of the melting enthalpy of 100 % homocrystalline PLLA that has a value of 106 J g^{-1}[16].

Thermogravimetric analysis

Thermal degradation was determined by thermal gravimetric analysis employing a TGA Q 500 equipment (TA Instruments). Approximately 3 mg samples were heated from room temperature to 800 °C at a rate of 10 °C min^{-1} under nitrogen flow of 100 mL min^{-1}.

Rheological measurements

The rheological measurements were carried out employing an ARG2 rheometer (TA Instrument) with parallel plates under nitrogen atmosphere. Continuous shear flow experiments were performed for all the samples at the same temperature gap from the glass transition temperature, but well above their melting peak.

Positron annihilation lifetime spectroscopy (PALS)

Positron lifetime spectra were recorded employing a conventional fast-fast nuclear spectrometer with a time resolution of 230 ps at room temperature. For each sample three spectra with 2 x 10^6 total counts were registered and analyzed employing

the PATFIT-88 program. ^{22}Na radioactive isotope was employed as a positron source that was prepared by depositing ^{22}NaCl between two Kapton foils. The positron source was placed between two identical samples that were 1 mm thick, in order to ensure that the annihilation of all the positrons occurs within the polymer [16].

The obtained spectra were fitted by employing three exponential decays and the longest component was associated with orthopositronium (*o*-Ps) lifetime. The positron annihilation lifetime, $\tau_{O-\mathrm{Ps}}$, can be correlated to the hole dimension and the hole radius, R, can be estimated by means of the Eldrup model following this equation [17],

$$\tau_{O-\mathrm{Ps}} = 0.5\left(1 - \frac{R}{R_0} + \frac{\sin 2\pi\frac{R}{R_0}}{2\pi}\right)^{-1} \text{(ns)} \quad (2)$$

where $R_0 = R + \Delta R$, ΔR is an empirical parameter, the best value is obtained by fitting all know data: 1.656 Å [18] and $\tau_{O-\mathrm{Ps}}$ is given in nanoseconds. The mean free volume hole size, V_H, can be calculated by the following equation assuming that the holes are spherical,

$$V_H = \frac{4\pi R^3}{3} \quad (3)$$

Employing PALS another parameter, the so-called relative intensity, $I_{O\text{-Ps}}$, can be obtained which is related to the number of the free-volume elements. Free volume fraction is obtained combining the size and number of free volume holes by means of this equation [19],

$$f = cV_H I_{O-\mathrm{Ps}} \quad (4)$$

where *c* is a constant characteristic of each material. Due to the difficulty to know the value of the constant for many polymers it has been defined another parameter: the apparent fractional free volume,

$$f_{app} = V_H I_{O-\mathrm{Ps}} \quad (5)$$

Although some authors state in literature that $I_{O\text{-Ps}}$ depends on the positron source activity, the thermal history of the samples and the composition and structure of the polymer, the apparent fractional free volume is widely accepted in literature [20].

Permeability characterization

Water vapour transmission rate was determined employing the permeation gravimetric cell. The cell is made of poly(tetrafluoroethylene) and it has two parts: the

first one is a small container partially filled with water. The membrane is placed on top of the cell and the other part closes the cell. The water vapour permeates trough the membrane and evaporates into the air. The cell is placed in a Sartorius analytical balance with a readability of 10^{-5} g and the weight loss is recorded in a computer for further data treatment. The measurements were performed at 25 °C and 30-60% relative humidity [5]. The values shown here are the average of at least 5 measurements. More details about the calculation of permeability can be found in the Supporting Information Note S1.

Oxygen permeability has been measured employing a Mocon Ox-Tran 2/21 MH model equipment. The measurements were performed at 23 °C, 1 atm and under dry conditions [5]. More details about the calculation of permeability can be found in the Supporting Information Note S1.

3. Results and Discussion

3.1. Characterization of the chain microstructure of LA-CL copolymers

The ring opening copolymerization of L-lactide and ε-caprolactone has been performed employing two different catalysts that have been proved to be efficient in this kind of copolymerization: stannous octoate ($SnOct_2$) and triphenyl bismuth (Ph_3Bi).

In Figure 1 the ^1H NMR of 50 LA 50 CL Ph_3Bi after 180 min reaction time is shown. For the calculation of the monomer conversion and microstructure characterization the signals at 5.17 ppm and 5.04 ppm, that correspond to the lactide methine of the L-lactide-co-ε-caprolactone (from now for the sake of clarity the monomer and copolymer will be labelled lactide and caprolactone) copolymer and of the monomer, respectively, were analysed. In the case of caprolactone the signals that appear at 4.0-4.3 ppm correspond to the methylene unit next to OCO. Specifically, the signal at 4.25 ppm corresponds to the CL monomer, 4.15 ppm signal corresponds to CL-LA dyad and 4.08 ppm to CL-CL dyad. The signals in the range of 2.3-2.7 ppm correspond to the methylene unit next to COO. More specifically, the signal at 2.66 ppm corresponds to the monomer, the signal at 2.42 ppm to CL-LA dyad and 2.32 ppm signal to CL-CL dyad. In the range of 1.2-1.9 ppm appear the signals corresponding to the protons of the methyl of LA and the protons of the three methylenes in the middle of CL. Also small traces of polyethylene from the caps of the NMR tube as well as

traces of water could be present in these signals, therefore, it is not highly recommended to use them taking into account that other signals are already available in the spectrum that allow a more reliable analysis [7,8].

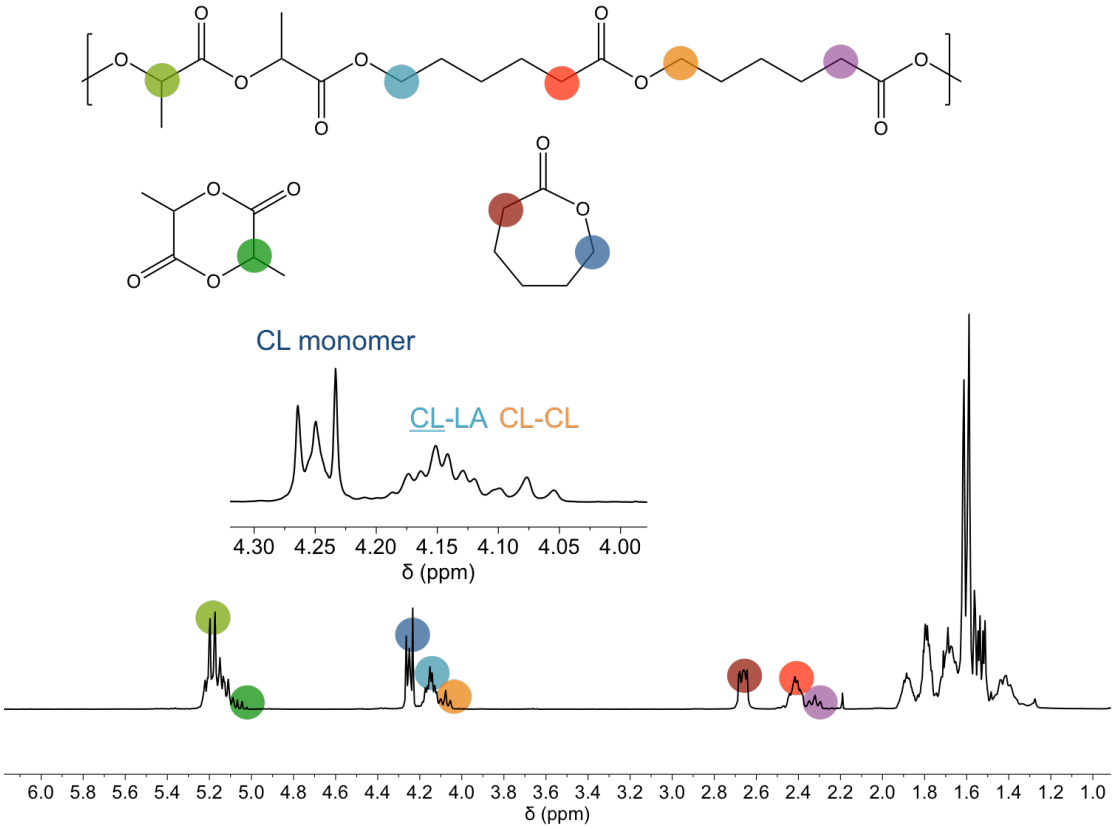

Figure 1. ^{1}H NMR spectra of 50 LA 50 CL Ph_3Bi copolymer after 180 min of reaction.

Figure 2 shows in the left the LA conversion in the copolymerization employing a) Ph_3Bi and c) $SnOct_2$ catalysts and in the right the CL conversion employing b) Ph_3Bi and d) $SnOct_2$ catalysts. As can be observed, lactide copolymerizes faster than caprolactone in both cases, regardless the catalyst employed. When Ph_3Bi is employed the conversion is very similar for the different feedings. On the other hand, when $SnOct_2$ is employed, after 25 min the conversion is lower for monomer feds rich in lactide. For both catalysts 100 % conversion of LA monomer is achieved after 100 min of reaction.

In the case of caprolactone, employing Ph_3Bi catalyst the polymerization rate decreases with increasing fraction of CL in the fed. The opposite trend is observed when $SnOct_2$ catalyst is used. The conversion of CL is in the range of 60-100 % obtaining higher conversions with $SnOct_2$ catalyst.

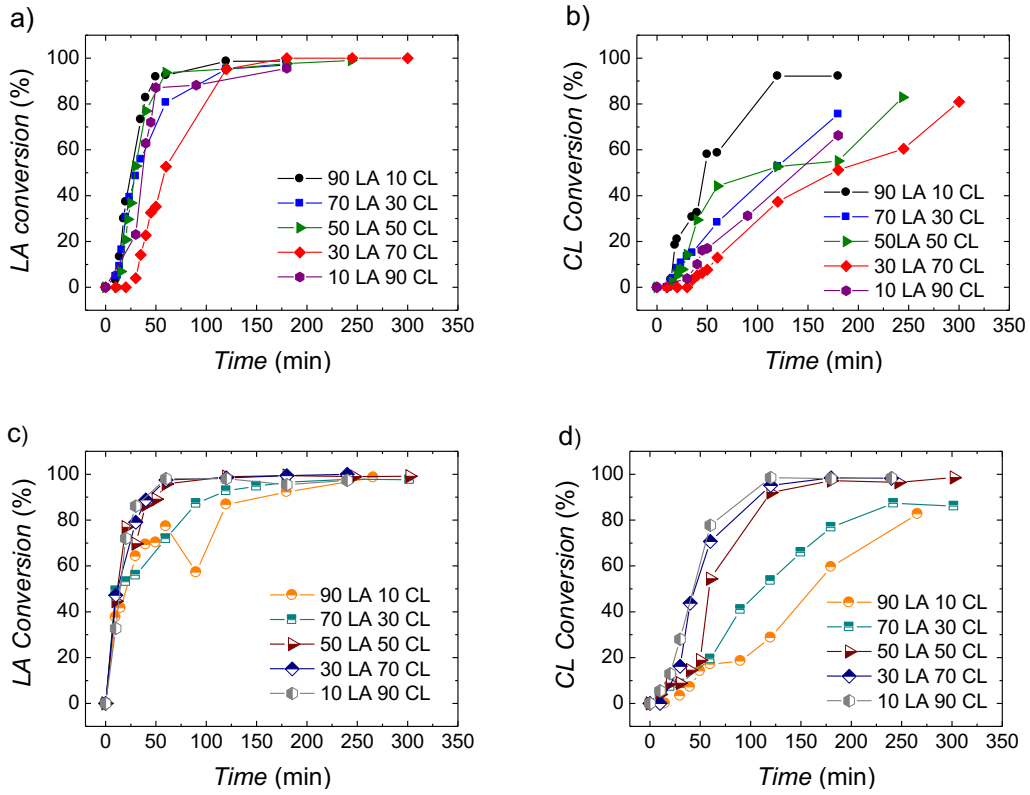

Figure 2. Monomer conversion evolution during reaction of a) lactide and b) caprolactone employing Ph_3Bi catalyst and c) lactide and d) caprolactone employing $SnOct_2$ catalyst.

In order to analyse better the differences between both catalysts in Figure 3 the conversion of lactide and caprolactone at 50 LA 50 CL monomer ratio employing a) Ph_3Bi and b) $SnOct_2$ catalysts are shown.

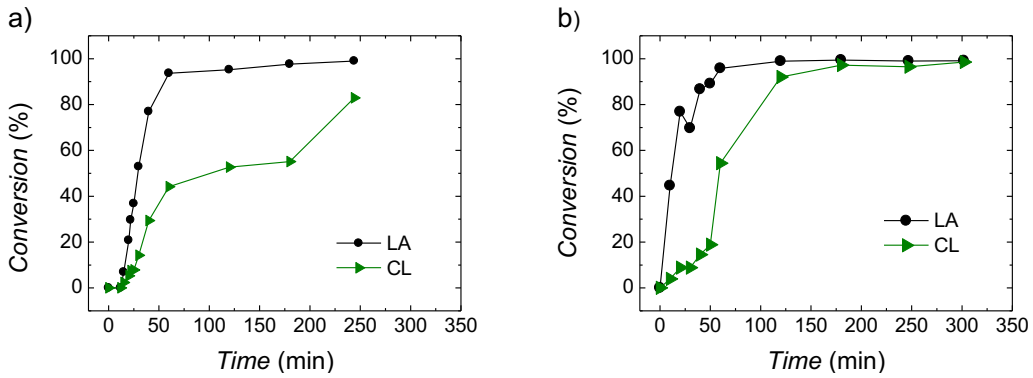

Figure 3. Monomer conversion of lactide and caprolactone with 50 LA 50 CL monomer feeding employing a) Ph_3Bi and b) $SnOct_2$ catalysts.

Lactide conversion achieves almost 100 % after a reaction time of 50 min; after this period of time caprolactone is incorporated to the copolymer chains, forming

"gradient" like structures. Therefore, the composition of the chains is richer in lactide at the beginning and richer in caprolactone at the end. The faster consumption of lactide monomer than caprolactone, which leads to the formation of gradient like or multiblock copolymers has been previously reported in literature [21]. In the case of the copolymers obtained with $SnOct_2$ catalyst, caprolactone incorporation at the end of the polymerization is higher than in the Ph_3Bi case.

The study of the chain microstructure of the copolymers over the whole reaction time sheds light on the evolution of the chain microstructure. To gain further insight into the chain microstructure of the copolymers, the average sequence lengths of LA and CL units have been calculated employing the following equations [22]:

$$l_{LA} = \frac{2(LA)}{(LA-CL)} \tag{6}$$

$$l_{CL} = \frac{2(CL)}{(LA-CL)} \tag{7}$$

$$\eta = \frac{(LA-CL)}{2(LA)(CL)} \tag{8}$$

where (LA) and (CL) are the two comonomer molar fractions, from now it will be expressed as cumulative composition, and (LA-CL) is the LA-CL average dyad relative molar fraction which is calculated employing this equation,

$$(LA-CL) = 2\left(\frac{(A_{2.32}+A_{4.15})/2}{A_{5.17}+\left(\frac{A_{2.32}+A_{2.42}+A_{4.15}+A_{4.25}}{2}\right)}\right) \tag{9}$$

where A_i is the integral of the signal at *i* shift. As can be seen in Figure 4 a-d the copolymers show a decreasing lactide unit length as a function of time, the length is longer for the copolymer richer in lactide monomer fed, as could be expected. In the case of caprolactone unit length, the value is near 1 at the beginning but with the reaction time it reaches higher values as the composition of the copolymer in caprolactone increases. However, these values have to be analysed with caution, since they provide an average value of the entire chain length.

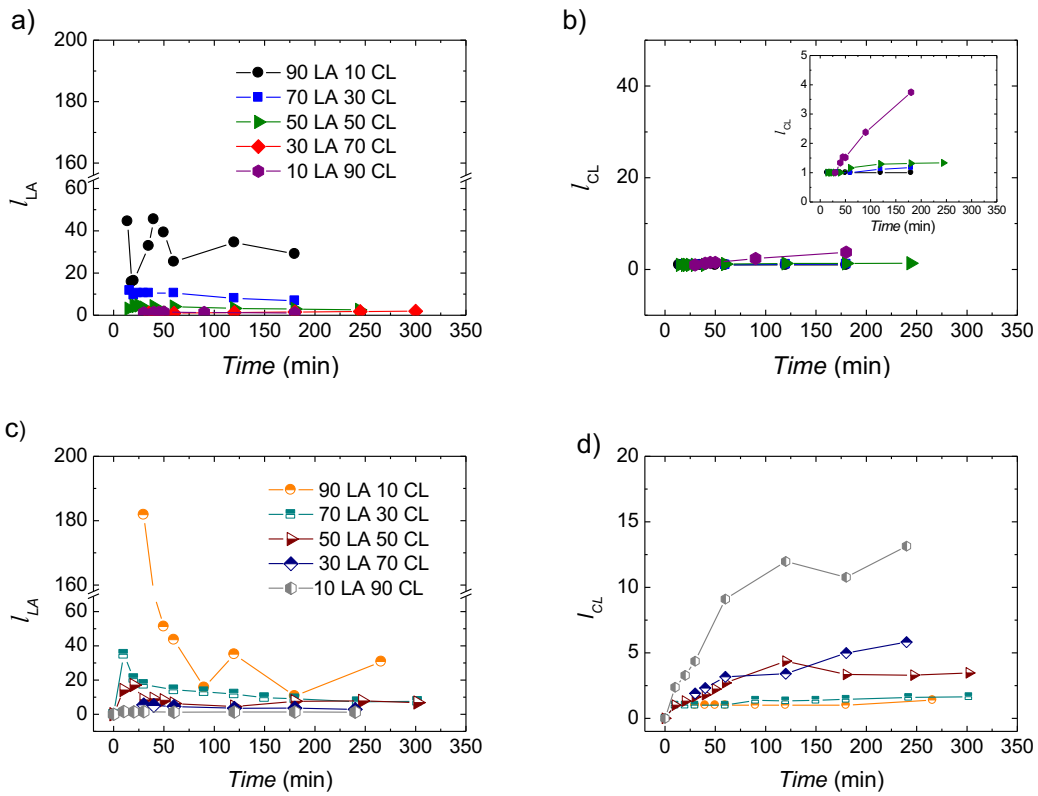

Figure 4. The number-average sequence lengths of a) lactide and b) caprolactone during reaction employing Ph_3Bi catalyst and c) lactide and d) caprolactone employing $SnOct_2$ catalyst.

Another important parameter to characterize the chain microstructure of the copolymer is the randomness character, η. When $\eta \to 0$ the copolymer shows block character, for $\eta \to 1$, random character and for $\eta \to 2$, alternant character [22]. In Figure 5 the randomness feature of the copolymers is shown. In the case of the copolymers obtained with Ph_3Bi catalyst, Figure 5 a, and copolymers rich in LA, the value of η is near 1 and is maintained practically constant during the reaction. In the case of copolymers rich in CL, initially higher values are obtained and as the reaction progresses η decreases to values close to 1. Thus, even though gradient like copolymers are obtained, in average they have random nature. For copolymers obtained with $SnOct_2$ catalyst, Figure 5 b, the value of η is near 1, except 50 LA 50 CL and 30 LA 70 CL where η decreases bringing about values close to 0.5.

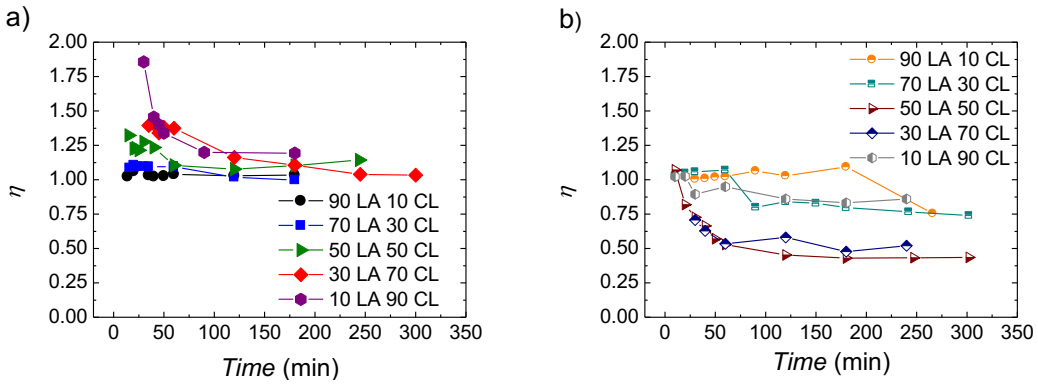

Figure 5. The randomness character during reaction employing a) Ph_3Bi and b) $SnOct_2$ catalyst.

In literature there are some works determining the reactivity ratio of this set of comonomers, although other catalysts and/or simple methods such as Kelen-Tudos and Mayo-Lewis methods have been employed [6,23]. To deepen into the copolymerization of lactide and caprolactone, the reactivity ratio of LA-CL system has been estimated using a nonlinear algorithm developed by de la Cal et al. [24], using $SnOct_2$ or Ph_3Bi catalysts (see Note S2 in Supplementary Information for more details).

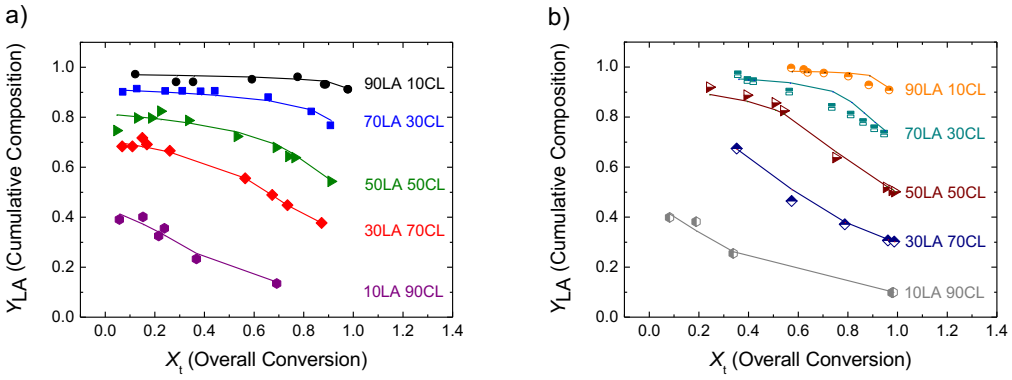

Figure 6. Conversion evolution of the cumulative composition of LA. Experimental results (dots) and model predictions (lines) for the estimated reactivity ratios for a) Ph_3Bi and b) $SnOct_2$ catalysts.

Figure 6 shows the comparison between the cumulative composition of LA determined experimentally by NMR analysis (dots) and the calculated cumulative compositions (lines) using the estimated reactivity ratios. The fittings of the cumulative composition for the experiments carried out at different monomer feds are quite good employing both, Ph_3Bi and $SnOct_2$ catalysts.

The reactivity ratios of each monomer employing different catalysts are shown in Table 1, where r_{LA} is the reactivity ratio of lactide and r_{CL} is the reactivity ratio of caprolactone. As it can be observed, lactide presents a higher reactivity ratio than caprolactone, which was expected, taking into account that lactide copolymerized faster than caprolactone (Figure 2). The reactivity ratio of lactide is 45 times higher than caprolactone with Ph_3Bi and 63 times higher with $SnOct_2$.

Table 1. Reactivity ratios of lactide and caprolactone employing Ph_3Bi and $SnOct_2$ catalysts.

Catalyst	r_{LA}	r_{CL}
Ph_3Bi	3.71 ± 0.34	0.082 ± 0.005
$SnOct_2$	11.48 ± 0.69	0.181 ± 0.005

Overall, the copolymers obtained with Ph_3Bi catalyst show less composition drift as compared to the case in which $SnOct_2$ catalyst was used, so Ph_3Bi catalyst has been selected to perform the polymerization at a larger scale and to study the physical properties. Eventually, one copolymer has been synthetized with $SnOct_2$ catalyst for comparison purposes.

3.2. Physico-chemical characterization of lactide-caprolactone copolymers synthetized in large scale

Chain microstructure characterization

After studying the synthesis of copolymers employing different catalysts, they were prepared at larger scale, selecting for that the adequate conditions and fed composition. Three copolymers were prepared with Ph_3Bi catalyst and another one with $SnOct_2$. In this section the composition and chain microstructure of these copolymers are analysed by ^1H NMR; the results are shown in Table 2. As can be seen, the copolymers obtained with Ph_3Bi catalyst show a random character and a long average lactide sequence length, as expected due to larger LA content. As the content on caprolactone increases the sequence length of lactide decreases significantly. The copolymers were also analysed by ^{13}C NMR obtaining very similar results comparing to ^1H NMR, see Figure S1 in Supporting Information. Furthermore, the ^{13}C NMR

analysis indicates that in the case of 73 LA 27 CL copolymer, there are isolated lactyl units, around 3 % (CL-L-CL instead of CL-LA-CL, where L and LA correspond to lactyl and lactide units, respectively). However, taking into account that the copolymer is rich in lactide it is possible that transesterification occurs at higher extent. In the case of the rest of copolymers the signal corresponding to isolated lactyl is not observed. In any case, as mentioned before, the copolymers are rich in lactide and transesterification can occur although it cannot be quantified.

93 LA 7 CL $SnOct_2$ copolymer shows a different behaviour with a randomness character of 0.65, which indicates that the copolymer shows apparently a multiblock character. However, from the previous kinetic experiments it is clear that the copolymers show a gradient like structure, being richer in lactide at the beginning and in caprolactone at the end of the polymerization reaction.

Table 2. Microstructure parameters obtained by ^{1}H NMR.

Sample	^{1}H NMR		
	l_{LA}	l_{CL}	η
96 LA 4 CL* Ph_3Bi	27.0	1.1	0.93
83 LA 17 CL Ph_3Bi	5.7	1.2	1.03
73 LA 27 CL Ph_3Bi	3.5	1.3	1.07
93 LA 7 CL $SnOct_2$	22.1	1.7	0.65

* Please note that, from now, Ph_3Bi was employed if the catalyst is not indicated.

Molar mass

The molar mass was determined by Size Exclusion Chromatography and the data obtained are shown in Table 3. PLLA has a molar mass of 256.3 kg mol^{-1}, calculated by GPC relative to poly(styrene) standards. In the case of the copolymers, as the incorporation of caprolactone increases the molar mass decreases; this may arise from the lower reactivity of caprolactone respect to lactide. For the obtained copolymers the dispersity index is between 1.6-1.7. In the case of PLLA the dispersity index is high (2.41), this value can be attributed to transesterification reactions.

Table 3. Weight average molar mass and dispersity index.

Sample	M_w[a] (Kg mol^{-1})	$Đ$[a]
PLLA[b]	256.3	2.41
96 LA 4 CL	145	1.70
83 LA 17 CL	93.7	1.67
73 LA 27 CL	48.6	1.61
93 LA 7 CL $SnOct_2$	80.9	1.77

[a] The molar mass was determined by GPC in tetrahydrofuran at 30 °C relative to poly(styrene) standards. [b]In the case of PLLA the molar mass was measured in chloroform.

Thermal properties

Since the glass transition temperature and the crystallinity degree play a crucial role on the transport properties, thermal properties were analysed. Table 4 shows the data obtained for the different copolymers.

The glass transition temperature has been analysed in the second DSC heating scan. All the samples show a broad glass transition temperature. Thermograms are shown in Supporting Information Figure S2. Neat PLLA shows a glass transition temperature of 55 °C, similar to the values reported in literature [25]. The incorporation of just 4 % of CL leads to a considerable reduction on the glass transition temperature giving rise to a value of 47 °C. The copolymers containing 17 % and 27 % of CL show low glass transition temperature values: 35 °C and 21 °C, respectively. In the case of 93 LA 7 CL $SnOct_2$ a glass transition temperature of 50 °C is obtained. The glass transition temperature of this copolymer is higher than that of 96 LA 4 CL copolymer obtained with Ph_3Bi. This probably arises from the fact that a more multiblock feature is obtained with $SnOct_2$.

In all the cases a single glass transition temperature is observed. Taking into account that the copolymers show a gradient like structure two glass transition temperatures could be expected: one corresponding to the lactide segments and another

one corresponding to the caprolactone segments. Although gradient like copolymers are obtained they are indeed rich in lactide, thus, even though caprolactone segments formed at the end of the polymerization should be larger than the average sequence lengths (1.1-1.7), it was not possible to detect the glass transition temperature corresponding to caprolactone segments.

The decrease of the T_g obtained for the copolymers is interesting, since it indicates that *a priori* a more ductile or elastomeric performance in terms of ductility can be expected.

Table 4. Melting temperature, T_m, crystallinity degree, X_c, and the crystallinity degree referred to lactide fraction in weight, $X_{c\,LA}$, obtained from the first DSC heating scan and glass transition temperature, T_g, obtained from the second scan, of PLLA and lactide-caprolactone copolymers.

Sample	T_g (°C)	T_m (°C)	X_c (%)	$X_{c\,LA}$ (%)
PLLA	55	177	34	34
96 LA 4 CL	47	149	21	22
83 LA 17 CL	35	127	10	12
73 LA 27 CL	21	108	11	15
93 LA 7 CL $SnOct_2$	50	165	35	38

The glass transition temperature has been theoretically calculated employing the additive rule:

$$T_g = T_{g1}w_1 + T_{g2}w_2 \qquad (10)$$

where T_g is the theoretical glass transition temperature, T_{g1} and T_{g2} are the glass transition temperatures of neat polymers and w_1 and w_2 are the weight fractions of each polymer.

Fox model [26] has also been employed to calculate the glass transition temperature:

$$\frac{1}{T_g} = \frac{w_1}{T_{g1}} + \frac{w_2}{T_{g2}} \qquad (11)$$

The results obtained by the additive rule and the Fox model are depicted in Figure 7. The additive rule estimates well the experimental glass transition temperature values obtained for the copolymers synthetized with Ph_3Bi catalyst. The Fox model underestimates the glass transition temperature and the values are far from the experimental results, which could arise from the fact that in this case gradient like copolymers are obtained, whereas Fox model is adequate for ideal Bernouillian random copolymers.

In Figure 7 the point corresponding to the copolymer obtained with $SnOct_2$ containing 7 % of CL is also presented. As it can be seen, it shows a higher glass transition temperature than the values predicted with both, the additive rule and Fox model. The different results obtained for the copolymers synthetized with the different catalysts arise from the observed distinct microstructures. As can be seen in Figure 4 the lactide segments are longer when $SnOct_2$ catalyst is employed, as comparing to the segments of the copolymers obtained with Ph_3Bi catalyst.

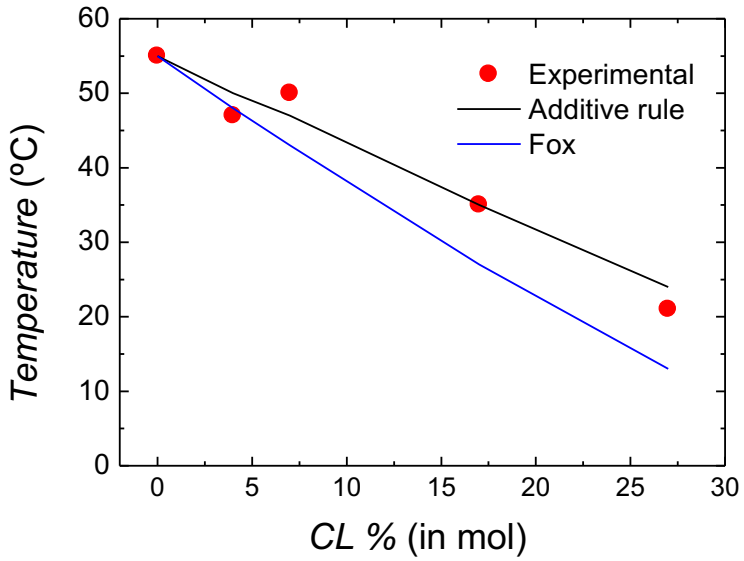

Figure 7. Glass transition temperature vs composition for the different lactide-caprolactone copolymers obtained. The data have been fitted to the equations 10 and 11.

The crystallinity of the samples was determined from the first DSC heating scans, see Figure 8. The melting temperature of neat PLLA is 177 °C; the incorporation of caprolactone decreases the melting temperature significantly and for 73 LA 27 CL copolymer a value of 108 °C is obtained. The melting temperature decrease arises from the presence of a second comonomer that reduces the length of the crystallizable chain segment. It is worthy to note that 83 LA 17 CL and 73 LA 27 CL show very broad melting peaks which can be attributed to the distribution of the crystal thickness, melting and recrystallization process and the formation of less perfect crystals. Moreover, taking into account that the copolymers show a gradient like structure the melting temperature of caprolactone could be eventually observed. However, since the selected copolymers are rich in lactide the caprolactone segments are not able to crystallize in these conditions. This is also confirmed by the limited crystallization ability of the lactide on the copolymers.

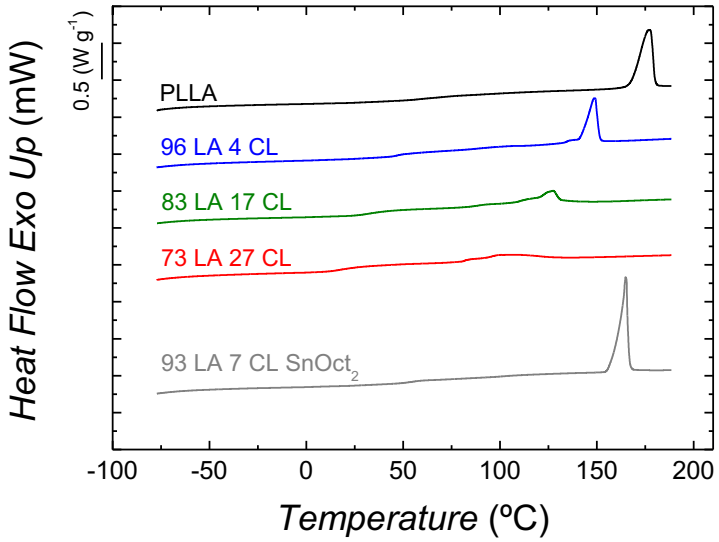

Figure 8. First DSC heating scans of PLLA and lactide-caprolactone copolymers.

The melting temperature of the copolymers can be predicted employing the following equation:

$$\Delta H_m^0 \left(\frac{1}{T_m} - \frac{1}{T_m^0}\right) = -R\ln X \qquad (12)$$

where ΔH_m^0 has been defined above, T_m is the melting temperature of the copolymer, $T_m^0 = 450$ K is the melting temperature of neat PLLA and X the molar fraction of lactide [27].

Figure 9 shows the experimental and theoretical melting temperature of lactide-caprolactone copolymers. All the copolymers synthetized with Ph_3Bi catalysts present a significantly lower melting temperature than the one predicted by the model. It is worthy to note that in the case of 93 LA 7 CL $SnOct_2$ copolymer the prediction matches perfectly the experimental result. These differences among the copolymers may arise again from the different microstructure: in the case of 93 LA 7 CL $SnOct_2$ copolymer a more multiblock character is obtained.

Noteworthy, the prediction of the glass transition temperature and melting temperature of the copolymers obtained with Ph_3Bi and $SnOct_2$ show their own trend. In the case of the T_g of the copolymers obtained with Ph_3Bi are between Fox and additive rule, whereas 93 LA 7 CL $SnOct_2$ is above these models. On the other hand, the melting temperature of 93 LA 7 CL $SnOct_2$ copolymer is well predicted whereas the copolymers obtained with Ph_3Bi show a significantly lower T_m than the predicted values.

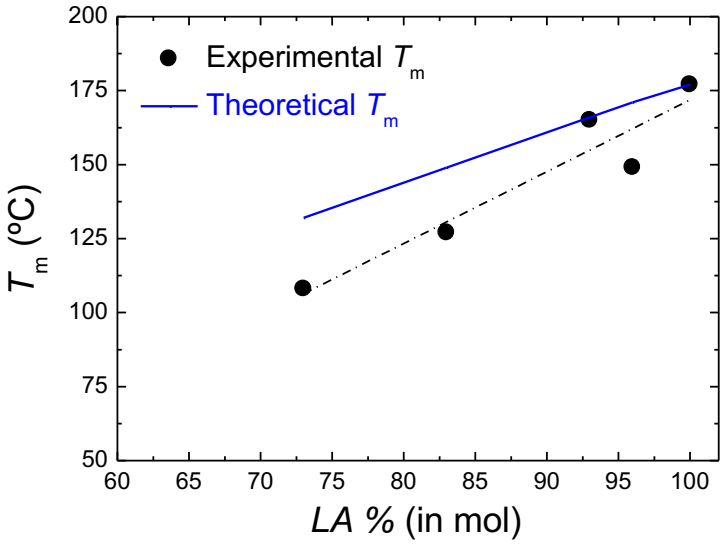

Figure 9. Experimental and theoretical melting temperatures of PLLA and lactide-caprolactone copolymers. The dashed line is to guide the eyes.

As mentioned previously the characterization of the crystallinity is of great importance since the crystalline regions are considered impermeable to gas and vapours. Actually, in these regions the penetrants can not solubilize and, in addition they create a tortuous pathway decreasing the diffusion coefficient and the overall permeability. The crystallinity degree of PLLA is 34 % and this value is decreased with

the incorporation of caprolactone: crystallinity degrees of 21 %, 10 % and 11 % are obtained for copolymers containing 4 %, 17 % and 27 % of caprolactone, respectively. Considering the effect of the composition of the copolymer, the incorporation of caprolactone hinders the crystallization of lactide segments giving rise to values of 22 %, 12 % and 15 % for the copolymers containing 4 %, 17 % and 27 % of CL, respectively. The copolymer with the lowest content on caprolactone shows a high crystallinity degree since the glass transition temperature is lower and this could enhance the crystallization ability of the polymer.

Regarding the copolymer obtained with the $SnOct_2$ catalyst, in particular 93 LA 7 CL copolymer, the crystallinity degree is similar to that of PLLA. On the basis of the composition of lactide, the crystallinity degree is even higher than neat PLLA. Once more, the differences between the copolymer obtained with $SnOct_2$ catalyst and the copolymers obtained with Ph_3Bi catalyst may arise from the lactide sequence length that is longer for the latter.

Furthermore, the rigid amorphous fraction of the samples has been estimated. For that, the specific heat change, Δc_p^0, is required, which corresponds to the fully amorphous sample, which has been previously reported for neat PLLA [25, 28, 29]. For the copolymers the value is not reported in literature, thus the value obtained from the second heating scan, which corresponds to amorphous sample, was employed. The obtained data are reported in Table S1 in Supporting Information. In all the cases the rigid amorphous fraction is very small, although this has to be analysed with caution since Δc_p^0 values do not follow a logical trend with the composition and the calculated values vary considerably if the chosen limits are slightly changed. Further studies are required to analyse soundly the rigid amorphous fraction.

The thermal stability during processing is of great importance taking into account that usually film blown extrusion is employed to obtain the films to be used for packaging applications.

As shown in Table 5, neat PLLA shows $T_{5\,\%}$ = 211 °C (temperature at which 5 % of weight is lost), which is an adequate thermal stability for film blown extrusion. The incorporation of caprolactone increases slightly this temperature, which makes the copolymers also suitable for the mentioned processing technique. The copolymer containing 27 % CL shows lower stability than expected; but, similar findings have

been found in literature for blends where the components influence each other stabilizing or destabilizing the system [30,31]. In the case of 83 LA 17 CL the stability is higher than expected, similar results have been observed in literature [14] however further studies are necessary to gain insight in the thermodegradation of lactide-caprolactone copolymers.

Table 5. Thermodegradation temperatures: $T_{5\%}$, temperature at which 5 % of weight is lost, and T_{max}, temperature of maximum degradation rate, of PLLA and lactide-caprolactone copolymers.

Sample	$T_{5\,\%}$ (°C)	T_{max} (°C)
PLLA	211	367
96 LA 4 CL	212	367
83 LA 17 CL	257	337
73 LA 27 CL	217	371
93 LA 7 CL $SnOct_2$	227	260

Rheological properties

Considering that the studied copolymers have potential applications in packaging, it becomes necessary to determine the rheological properties that affect to the processing of the material. For that purpose, the rheological behaviour of PLLA and different copolymers has been studied under continuous shear flow. The obtained results are presented in Figure 10. The effect of temperature on the viscosity, owed to

the increase of the free volume with respect to the iso-free state at $T = T_g$, is minimized taking the same temperature gap from the glass transition temperature of each copolymer. This allows focusing on the respective effects of the microstructure and the composition of the copolymers and molar mass.

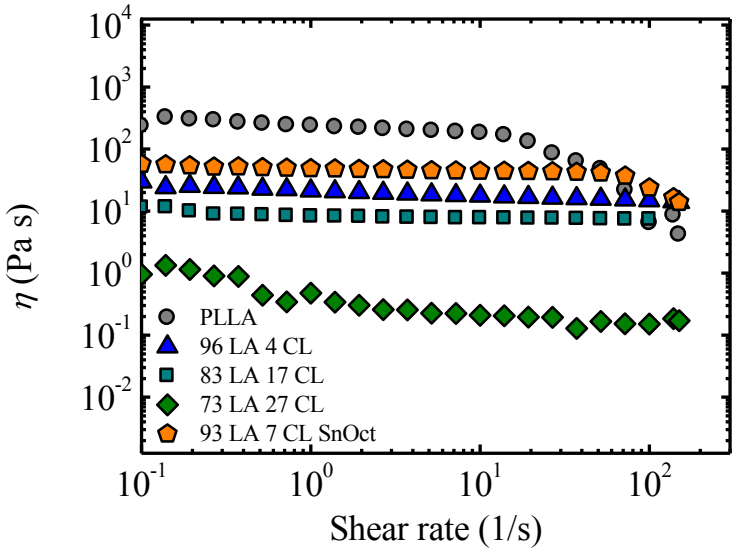

Figure 10. Viscosity of PLLA and lactide-caprolactone copolymers as a function of shear rate at the same temperature gap from the glass transition temperature (see Table 4).

As mentioned in the characterization section, the molar mass of the copolymers is reduced as the amount of CL is increased, except in the case of 93 LA 7 CL $SnOct_2$ copolymer which deviates from the general trend, because of its multiblock character. Consequently, a decrease of the viscosity with the amount of CL is observed in Figure 10, except for 93 LA 7 CL $SnOct_2$ sample, for which the particular microstructure can play a significant role enhancing viscosity. In literature the rheological properties of block copolymers have been widely studied [32-36], demonstrating that they give rise to a higher viscosity than random copolymers of similar molar weight.

With the aim of separating the effect of the molar mass from the contribution of the amount of CL and microstructure, the viscosity of the copolymers has been theoretically calculated employing molecular characteristic parameters of both LA and CL monomers.

For that purpose an analysis of the polymer chain entanglements is carried out. The entanglements plateau modulus is calculated employing two different equations, one derived from the theory of rubber elasticity and the other based on the chemical structure of the monomer, as it is explained in the following lines.

When the theory of the entropic elasticity of crosslinked rubbers is considered, the following expression is obtained for the entanglement plateau modulus [37]:

$$G_N^0 = \frac{\rho RT}{M_e} \tag{13}$$

being M_e the molar mass between entanglements, ρ the density of the melt, R the gas constant and T the temperature.

On the other hand, the study of a significant number of polymers by Fetters [38] lead to establish the following equation to calculate the entanglement plateau modulus based on the characteristic parameters of the monomer [38,39],

$$G_N^0 = k\left(\frac{C_\infty l_0^2 N_A \rho}{m_0}\right) \tag{14}$$

being C_∞ the characteristic ratio, l_0 the average backbone bond length, m_0 the average molar mass per backbone bond, N_A the Avogadro number and k a constant.

Combining both equations and the following values [40] for PLLA: M_e = 8000 g mol^{-1}, ρ = 1.09 g cm^{-3}, C_∞ = 10.5, l_0 = 1.46 Å and m_0 = 24 g mol^{-1}, a value of k = 2.24x10^{-24} kg m^{-2}s^{-2} is obtained.

Above the critical molar mass for entanglements the Newtonian viscosity can be expressed in terms of the entanglements density M_w/M_e:

$$\eta_0 = k'\left(\frac{M_w}{M_e}\right)^{3.4} \tag{15}$$

being η_0 Newtonian viscosity, k' a constant and M_w the weight average molar mass of the samples and M_e the molar mass between entanglements. From this equation a value of k' = 2.29 x 10^{-3} Pa s is obtained for PLLA.

To calculate the viscosity corresponding to each copolymer, the characteristic parameters of the copolymers are first calculated, assuming a linear variation with the amount of PCL. For that, the following values for PCL are considered [41]: M_e = 1600 g mol^{-1}, ρ = 1.20 g cm^{-3}, C_∞ = 5.56, l_0 = 1.51 Å and m_0 = 16.3 g mol^{-1}.

Using the characteristic parameters, the corresponding entanglements moduli are obtained (Equation 14) and then the entanglements molar mass to calculate the entanglements densities, M_w/M_e, and the theoretical viscosity values (Table 6).

The experimental values of the viscosity of Figure 10 have been compared to the theoretical ones obtained employing the mentioned equations, in order to ascertain the differences in the results between both procedures. Comparing the experimental and theoretical viscosity values, it is seen that for 83 LA 17 CL and 73 LA 27 CL compositions the matching is good. However, for the copolymers rich in LA the agreement is not good. Considering the analysis of the microstructure of the copolymer explained before, this mismatch for the copolymer rich in LA can be explained taking into account that they show a more gradient like structure comparing with copolymers with higher CL content. In addition, the copolymer obtained with $SnOct_2$ shows a more blocky character since the randomness character deviates significantly from 1.

Table 6. Experimentally obtained viscosity values and theoretically calculated ones considering different molar masses for PLLA and LA-CL copolymers at the indicated temperatures. M_e values are obtained as indicated in the text.

Material	$T=T_g+100$	M_e (g mol^{-1})	M_w (g mol^{-1})	η_{exp} (Pa s)	η_{theo} (Pa s)	η_{theo,M_w} [a] (Pa s)
PLLA	192	8000	256300	302.7		
96 LA 4 CL	184	8019	145000	29.7	42.9	299.6
83 LA 17 CL	172	8116	93700	11.4	9.3	287.5
73 LA 27 CL	158	8236	48600	0.96	0.95	273.6
93 LA 7 CL $SnOct_2$	187	8036	80900	57.1	5.86	297.4

[a] considering in all cases $M_w = 256300$ g mol^{-1}.

As it has been mentioned previously, in order to separate the effect of CL comonomer from the effect of the molar mass, the viscosity of the copolymers has been calculated considering the same molar mass as PLLA homopolymer. The values are shown in Table 6. It can be observed that the viscosity is reduced with the incorporation of CL but this reduction is less severe than in the case of the experimental values which

include both effects. For PLLA 302.7 Pa s is obtained experimentally, for 96 LA 4 CL sample 299.6 Pa s is obtained theoretically, whereas for the copolymer with the highest content of CL, 73 LA 27 CL, a value of 273.6 Pa s is obtained theoretically. These results indicate that considering the same molar mass the incorporation of 27 % CL reduces the viscosity only about 10 %. These results reflect that the main factor governing the viscosity of the copolymers is the molar mass rather than the composition. Therefore, the molar mass can be used to fine tune the viscosity; a lower viscosity can facilitate the processing and bring down the energy consumption.

Characterization of the free volume

The importance of the free volume fraction on transport properties has been extensively reported in the literature [25,42]. The free volume of the samples has been characterized by positron annihilation lifetime spectroscopy (PALS). PALS spectra of each sample are shown in Supporting Information Figure S3.

Figure 11 shows the *ortho*-positronium lifetime ($\tau_{o\text{-Ps}}$) and the relative intensity ($I_{o\text{-Ps}}$) of PLLA and copolymers; the data is reported in Table S2 in Supporting Information. The 73 LA 27 CL copolymer was not measured due to experimental problems related to its elastomeric state at room temperature.

Poly(lactide) shows the highest *ortho*-positronium lifetime, $\tau_{o\text{-Ps}}$, (1984 psec), which corresponds to the highest free volume hole size. In the case of the copolymers the incorporation of just 4 % of caprolactone reduces the *ortho*-positronium lifetime (1959 psec), but for the copolymer containing 17 % of caprolactone not a significant change is observed (1957 psec). Therefore, the incorporation of caprolactone mantains or even reduces the free volume hole size.

The relative intensity, $I_{O\text{-Ps}}$, which is related to the free volume hole number, as mentioned previously, is equal to 15.6 % for PLLA. In the case of copolymers the incorporation of caprolactone increases the intensity, for 4 % of caprolactone $I_{O\text{-Ps}}$ = 16.5 % is obtained and for 17 % of caprolactone $I_{O\text{-Ps}}$ = 16.9 %. It can be deduced that the incorporation of caprolactone increases the free volume hole number, notwithstanding this increase is not proportional to the composition of the copolymer.

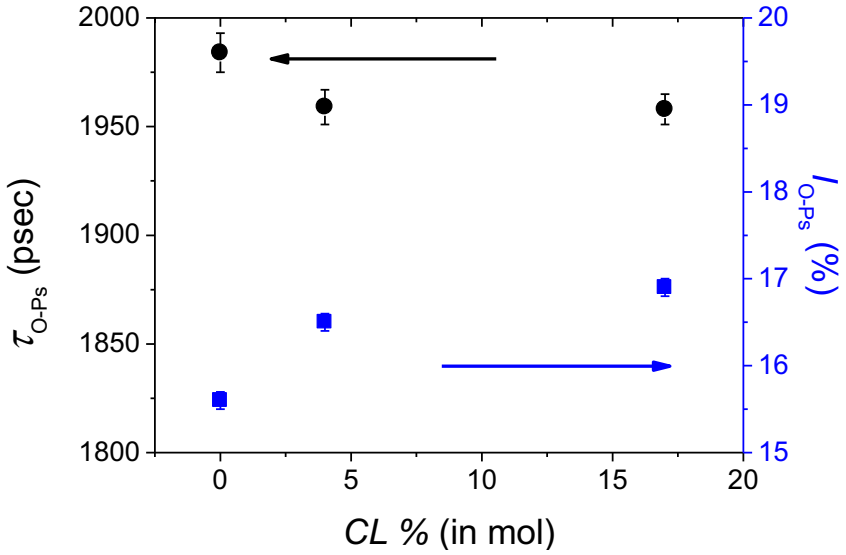

Figure 11. *Ortho*-positronium lifetime ($\tau_{o\text{-}Ps}$) and relative intensity ($I_{o\text{-}Ps}$) of PLLA and lactide-caprolactone copolymers.

The apparent fractional free volume, f_{app}, encompasses both, the free volume hole size and number, and it is shown in Figure 12 in arbitrary units (see Table S2 in Supporting Information). PLLA shows the lowest apparent free volume fraction (1487 a.u.) and as the content on caprolactone increases the apparent fractional free volume rises. This increase is lower than expected, specially in the case of the copolymer containing 17 % of caprolactone, recalling that the incorporation of caprolactone reduces the glass transition temperature (see Figure 7).

Other polyesters show a similar behaviour, for example in PBAT/PH blends [42], where the incorporation of PH reduces the free volume hole size but increases the free volume hole number. Note that in the case of LA-CL copolymers the changes are more subtle (free volume fraction values in the range of 1484-1568 a.u.) than in the PBAT/PH system for which the free volume fraction lie in the range 2249-1769 a.u. In other polymer systems such as polymer blends [42,43], polymer-plasticizer blends [44] and copolymers [45] the free volume fraction change is more significant.

These results indicate that the incorporation of caprolactone does not increase significantly the free volume fraction, which will be reflected in the permeability results shown below.

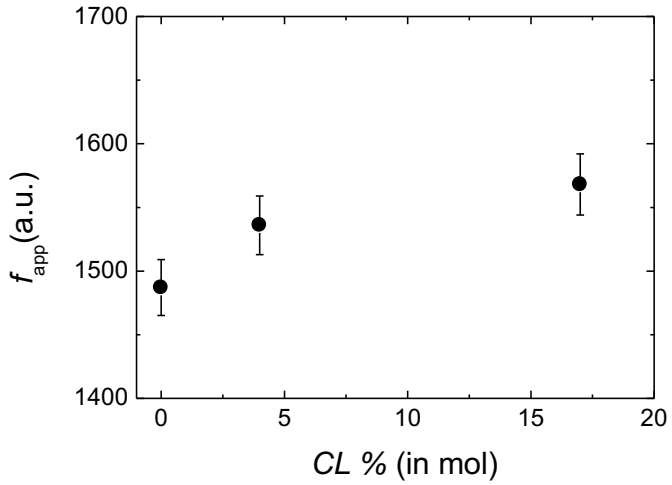

Figure 12. Apparent free volume fraction of PLLA and lactide-caprolactone copolymers.

Oxygen permeability

Oxygen permeability has been measured for PLLA and LA-CL copolymers since oxygen can provoke physical and chemical changes deteriorating food [39]. In Figure 13, see the data in Table S3 in Supporting Information, it can be seen that neat PLLA presents an oxygen permeability value of 0.25 Barrer, which is in the range of the values reported for PLLA before [25]. The copolymer with 7 % CL shows a similar permeability compared to PLLA, with a value of 0.24 Barrer. For the copolymers containing 17 % and 27 % caprolactone, respectively, the permeability rises considerably, especially for the latter which shows a value of 0.62 Barrer. However, this value is still lower than that of neat PCL which has an oxygen permeability of 0.88 Barrer [43]. The oxygen permeability of copolymers increases with the increasing content of caprolactone, which is compatible with the observed decrease of the glass transition temperature and crystallinity, as well as the increase of free volume fraction. Taking into account the small increase of the free volume, it could be deduced that the thermal properties play a relevant role.

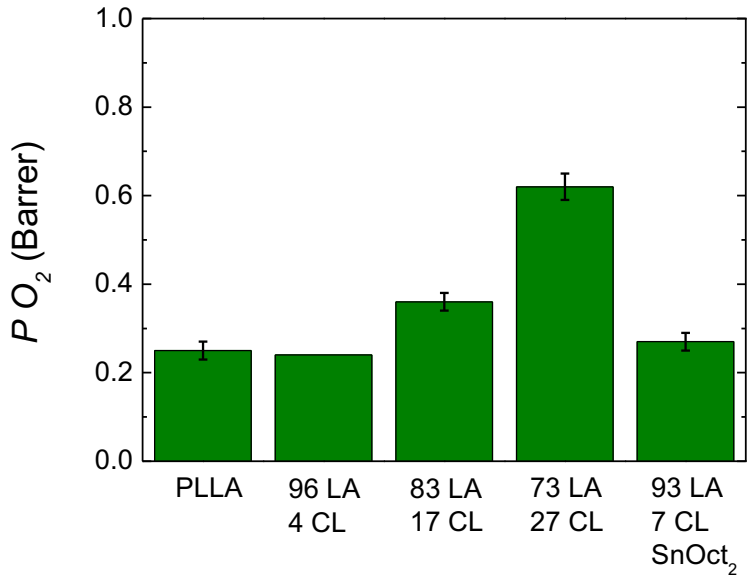

Figure 13. Oxygen permeability of lactide-caprolactone copolymers.

Water vapour transmission rate

The characterization of water vapour is of great importance since water can cause chemical and physical changes deteriorating food [42]. Water vapour transmission rate (*WVTR*) of PLLA and LA-CL copolymers was measured and the values are depicted in Figure 14; the data are reported in Table S3 in Supporting Information.

Neat PLLA shows a value of 4.9 g mm m^{-2} day^{-1} which is similar to the values reported in literature, for example in a previous work we reported a value of 5.9 g mm m^{-2} day^{-1} [25]. In the case of the copolymers, the incorporation of caprolactone decreases the *WVTR* significantly: with the incorporation of 4 and 17 % CL, 3.73 g mm m^{-2} day^{-1} and 3.70 g mm m^{-2} day^{-1} are obtained, respectively. On the other hand, the incorporation of 27 % CL leads to a higher water vapour transmission rate than neat PLLA. It is also worthy pointing that, according to our previous study [5], commercial poly(ε-caprolactone), with a value of 11.3 g mm m^{-2} day^{-1}, presents a water vapour transmission rate that is higher than that of poly(lactide).

Taking into account that the incorporation of caprolactone decreases the glass transition temperature as well as the crystallinity degree of copolymers and that PCL shows a higher water vapour transmission rate than PLLA, it would be expected that copolymers would show a higher permeability than neat PLLA. However, this is not the observed trend and permeability values are lower than the values obtained theoretically from additive rule.

The different behaviour observed for water vapour compared to oxygen can be attributed to the nature of water: it can interact strongly through hydrogen bonds and dipole-dipole interactions, whereas oxygen can form only weak Van der Waals interactions. Furthermore, water molecules tend to form clusters which decrease the diffusion coefficient and therefore the overall permeability. In fact clustering phenomena in PLLA has been reported before [44] and it is likely that this clustering tendency may be higher in the copolymers. Also, the balance of interactions between lactide and caprolactone moieties and water molecules can lead to the reduction of *WVTR*. Additionally, the large increase found for 73 LA 27 CL can be attributed to the fact that the copolymer is in elastomeric state, overcoming the effect of the reduction of the interactions between water and copolymer and the clustering trend.

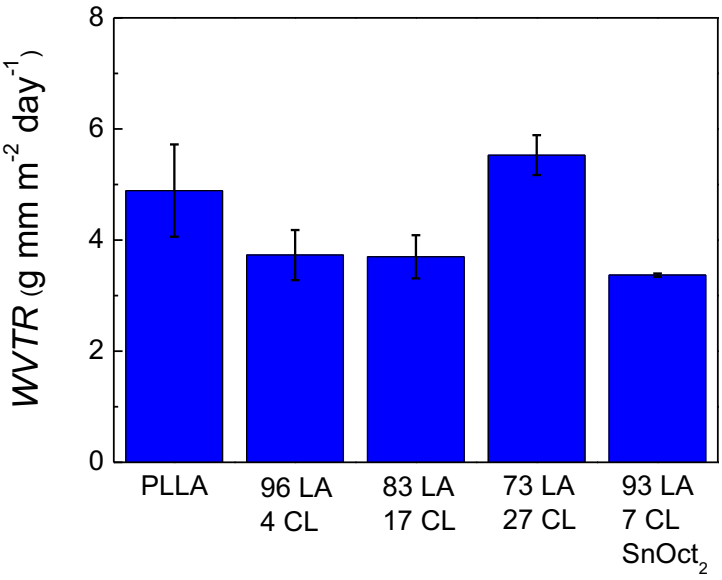

Figure 14. Water vapour transmission rate of lactide-caprolactone copolymers.

As compared to other commercial biodegradable polymers, these copolymers present a better barrier character than neat poly(caprolactone). The oxygen permeability of the copolymers is slightly higher than that of neat PLLA [43]. The water vapour transmission rate is similar or lower than neat PLLA, depending on the composition, therefore they could be interesting to replace PLLA since they present a lower glass transition temperature and probably a better ductility [7,8], which is one of the major drawbacks to use PLLA in the packaging sector. It has been reported that poly(hydroxybutyrate) shows excellent barrier properties, notwithstanding its ductility is low [46]; this has been solved by the synthesis of copolymers of hydroxyvalerate

with tuned properties [47]. Our lactide-caprolactone copolymers show moderate permeability to oxygen and water vapour and are suitable for those packaging applications where a high barrier character is not a requirement.

Overall, lactide-caprolactone copolymers present an interesting strategy to broaden the use of biodegradable materials in packaging. The ring opening copolymerization of lactide and caprolactone can be performed easily and the adequate selection of the composition allows obtaining materials with convenient thermal and barrier properties. Thus, depending on the application the most adequate composition can be selected**.**

Conclusions

L-Lactide-co-ε-caprolactone copolymers were obtained by $SnOct_2$ and Ph_3Bi catalysts in order to study their suitability for packaging applications. With this aim the synthesis of the copolymers, their characterization and the thermal properties, free volume and permeability have been studied.

It has been observed that $SnOct_2$ catalyst leads to copolymers that show a gradient like feature, whereas in the case of Ph_3Bi based copolymers, the gradient like character is less pronounced. The study of the kinetics of the copolymerization sheds light on the evolution of the chain microstructure during the reaction, where it is observed that although at the end apparently random character is obtained for copolymers obtained with Ph_3Bi catalyst they show a multiblock character. Furthermore, the reactivity ratios have been calculated observing that lactide reactivity is much higher than that of caprolactone, which favours gradient like copolymers.

The characterization of the physical properties of the copolymers shows that the incorporation of small amounts of caprolactone reduces considerably the glass transition temperature, the melting temperature and the crystallinity degree. Regarding the barrier character, in the case of oxygen permeability, the addition of CL increases gradually the permeability showing moderate values. On the other hand, water vapour transmission rate shows the opposite behaviour: the permeability is decreased with the content of CL for copolymers containing up to 17 % CL. These results indicate that, in this case, the interactions between water and polymer play a more relevant role than the free volume and thermal properties. Overall, by selecting the adequate composition and

catalyst it is possible to obtain materials *ad hoc* for each application fulfilling the specific requirements. Thus, these copolymers perform differently to broaden the applications of polylactide, particularly in packaging.

CRediT authorship contribution statement

Ainara Sangroniz: Conceptualization, methodology, data curation, formal analysis, writing, review & editing. **Leire Sangroniz**: Data curation, writing-review & editing. **Shaghayegh Hamzehlou**: Data curation, review & editing. **Javier del Río**: Data curation. **Antxon Santamaria** Review & editing. **Jose Ramon Sarasua:** Conceptualization, review and editing. **Marian Iriarte**: Conceptualization, methodology, supervision, writing-review & editing. **Jose Ramon Leiza**: Methodology, review & editing. **Agustin Etxeberria**: Conceptualization, methodology, supervision, writing- review & editing.

Declaration of competing interest

The authors declare that they have no known competing financial interests or personal relationships that could have appeared to influence the work reported in this paper.

Acknowledgements

The authors are grateful to the financial support from the Basque Government (GC IT-1313-19, GC IT-1309-19 and GC IT-999-16) and the Spanish Ministry of Innovation and Competitiveness MINECO (MAT-2016-78527-P). A. Sangroniz thanks the Basque Government for the PhD grant. S. Hamzehlou acknowledges the University of the Basque Country (UPV/EHU) for the "Contratación para la especialización de personal investigador doctor" postdoctoral grant. The authors thank the technical and human support provided by Sofia Guezala (NMR SGIker) and European Funding (ERDF and ESF).

References

1. PlasticsEurope, Plastics The Facts: An analysis of European plastics production, demand and waste data (PlasticsEurope, 2018).
2. R.A. Gross, B. Kalra, Biodegradable polymers for the environment, Green Chem., 297 (2002), 803-807.
3. U. Sonchaeng, F. Iñiguez-Franco, R. Auras, S. Selke, M. Rubino, L.T. Lim, Poly(lactic acid) mass transfer properties, Prog. Polym. Sci., 86 (2018), 85-121.
4. J. Fernández, H. Amestoy, A. Larrañaga-Varga, H. Sardon, M. Aguirre, J. R. Sarasua, Effect of molecular weight on the physical properties of poly(ethylene brassylate) homopolymers, J. Mech. Behav. Biomed. Mater., 64 (2016), 209-219.
5. A. Sangroniz, J.R. Sarasua, M. Iriarte, A. Etxeberria, Survey on transport properties of vapours and liquids on biodegradable polymers, Eur. Polym. J., 120 (2019), 109232.
6. A. Polyakova, R.Y.F. Liu, D.A. Schiraldi, A. Hiltner, E. Baer, Oxygen-barrier properties of copolymers based on ethylene terephthalate, J. Appl. Polym. Sci., 39 (2001) 1889-1899.
7. J. Fernández, A. Etxeberria, J.M. Ugartemendia, S. Petisco, J.R. Sarasua, Effects of chain microstructures on mechanical behavior and aging of a poly(L-lactide-*co*-caprolactone) biomedical thermoplastic-elastomer, J. Mech. Behav. Biomed., 12 (2012), 29-38.
8. J. Fernández, A. Etxeberria, J.R. Sarasua, Synthesis, structure and properties of poly(L-lactide-*co*-caprolactone) statistical copolymers, J. Mech. Behav. Biomed., 9 (2012), 100-112.
9. L. Mezzasalma, J. De Winter, D. Taton, O. Coulembier, Benzoic acid organocatalyzed ring-opening (co) polymerization (ORO(c)P) of L-lactide and ε-caprolactone under solvent-free conditions: from simplicity to recyclability, Green Chem., 20 (2018), 5385.
10. L. Mezzasalma, S. Harrison, S. Saba, P. Loyer, O. Coulembier, D. Taton, Bulk organocatalytic synthetic access to statistical copolyesters from L-lactide and ε-caprolactone using benzoic acid, Biomacromolecules, 20 (2019), 1965-1974.
11. R.M. Slattery, A.E. Stahl, K.R. Brereton, A.L. Rheingold, D.B. Green, J.M. Fritsch, Ring opening polymerization and copolymerization of L-lactide and

ε-caprolactone by bis-ligated magnesium complexes, J. Polym. Sci. Part A, 57 (2019), 48-59.

12. T. Shi, W. Luo, S. Liu, Z. Li, Controlled random copolymerization of rac-lactide and ε -caprolactone by well-designed phenoxyimine Al complexes, J. Polym. Sci. Polym. Chem., 56 (2018), 611-617.
13. H.R. Kricheldorf, Syntheses of biodegradable and biocompatible polymers by means of bismuth catalysts, Chem. Rev., 109 (2009), 5579-5594.
14. J. Fernández, A. Etxeberria, JR. Sarasua, Effects of repeat unit sequence distribution and residual catalyst on thermal degradation of poly(l-lactide/ε-caprolactone) statistical copolymers, Pol. Degrad. Stab. 98 (2013) 1293-1299
15. J. Fernández, E. Meaurio, A. Chaos, A. Etxeberria, A. Alonso-Varona, J.R. Sarasua, Synthesis and characterization of poly(L-lactide/ε-caprolactone statistical copolymers with well resolved chain microstructures, Polymer, 54 (2013), 2621-2631.
16. J. del Río, A. Etxeberria, N. López-Rodríguez, E. Lizundia, J.R. Sarasua, A PALS contribution to the Supramolecular Structure of Poly(L-lactide), Macromolecules, 43 (2010), 4698–4707.
17. M. Eldrup, D. Lightbody, J.N. Sherwood, Temperature dependence of positron lifetimes in solid pivalic acid, Chem. Phys., 63 (1981), 51–58.
18. H. Nakanishi, S.J. Wang, Y.C. Jean, Positron Annihilation Studies of Fluids, World Scientific, Singapore, 1988, 285–291.
19. Y.Y. Wang, H. Nakanishi, Y.C. Jean, T.C. Sandreczki, Positronium formation at free volume sites in the amorphous regions of semicrystalline PEEK, J. Polym. Sci. B: Polym. Phys., 27 (1990), 1419–1424.
20. C.L. Wang, T. Hirade, F.H.J. Maurer, M. Eldrup, N.J. Pedersen, Free-volume distribution and positronium formation in amorphous polymers: temperature and positron-irradiation-time dependence, J. Chem. Phys., 108 (1998), 4654–4661.
21. M. Florczak, A. Duda, Effect of the configuration of the active center on comonomer reactivities: the case of ε-caprolactone/L,L-lactide copolymerization, Angew. Chem. Int. Ed., 47 (2008), 9088-9091.
22. R.N. Ibbet, NMR Spectroscopy of Polymers Ch. 2 (Blackie Academic & Professional, London, 1993).

23. F. Faÿ, E. Renard, V. Langlois, I. Linossier, K. Vallée-Rehel, Development of poly(ε-caprolactone-*co*-L-lactide) and poly(ε-caprolactone-*co*-δ-valerolactone) as new degradable binder used for antifouling paint. Eur. Polym. J., 43 (2007), 4800-4813.
24. J.C. De La Cal, J.R. Leiza, J.M. Asúa, Estimation of reactivity ratios using emulsion copolymerization data, J. Polym. Sci. Part A Polym. Chem., 29 (1991), 155–167.
25. A. Sangroniz, A. Chaos, M. Iriarte, J. del Río, J.R. Sarasua, A. Etxeberria, Influence of the rigid amorphous fraction and crystallinity on polylactide transport properties, Macromolecules, 51 (2018), 3923-3931.
26. O. Olabisi, L.M. Robeson, M.T. Shaw, Polymer-polymer Miscibility, Academic Press, New York, 1979.
27. J.R. Sarasua, R.E. Prud´homme, M. Wisniewski, A. Le Borgne, N. Spassky, Crystallization and melting behaviour of polylactides, Macromolecules, 31 (1998), 2895-3905.
28. J. Del Río, A. Etxeberria, N. López-Rodríguez, E. Lizundia, J.R. Sarasua, A PALS contribution to the supramolecular structure of poly(L-lactide), Macromolecules, 43 (2001), 4698-4707.
29. E. Zuza, J.M. Ugartemendia, A. Lopez, E. Meaurio, A. Lejardi, J.R. Sarasua, Polymer, Glass transition behavior and dynamic fragility in polylactides containing mobile and rigid amorphous fractions, 49 (2008), 4427-4432.
30. J.I. Eguiazábal, J.J. Iruin, Miscibility and thermal descomposition in phenoxy/poly(ethylene terephthalate) and phenoxy/poly(butylene terephthalate) blends, Mater. Chem. Phys., 18 (1987), 147–154.
31. A. Sangroniz, L. Sangroniz, N. Aranburu, M. Fernandez, A. Santamaria, M. Iriarte, A. Etxeberria. Blends of biodegradable poly(butylene adipate-co-terephthalate) with poly(hydroxi amino ether) for packaging applications: Miscibility, rheology and transport properties. Eur. Polym. J., 105 (2018), 348-358.
32. F.S. Bates, Block copolymers near the microphase separation transition. 2. Linear dynamic mechanical properties, Macromolecules, 17 (1984), 2607-2613.

33. J.H. Rosedale, F.S. Bates, Rheology of ordered and disordered symmetric poly(ethylenepropylene)-poly(ethylethylene) diblock copolymers, Macromolecules, 23 (1990), 2329-2338.
34. C.D. Han, J. Kim, Rheological technique for determining the order-disorder transition of block copolymers, J. polym. Sci. B Polym. Phys., 25 (1987), 1741-1764.
35. J.C. Majesté, A. Santamaria, Rheology and viscoelasticity of multiphase polymer systems: Blends and block copolymers. In Handbook of multiphase polymer systems. A. Boudenne, L. Ibos, Y. Candau, S. Thomas, John Wiley & Sons Chichester 2011.
36. G.V. Vinogradov, A.Y. Malkin, "Rheology of Polymers" Springer Berlin Heidelberg 1980.
37. J.D. Ferry, Viscoelastic properties of polymers. John Wiley & Sons New York 1980.
38. L.J. Fetters, D.J. Lohse, R.H. Colby, Chain dimensions and entanglement spacings. J. E. Mark Ed, in Physical Properties of Polymer Handbook.
39. W.W. Graessley, Entangled Chain Dynamics in Polymer Liquids and Networks: Dynamics and Rheology Garland Science, London 2008.
40. J.J. Cooper-White, M.E. Mackay, Rheological properties of poly(lactides). Effect of molecular weight and temperature on the viscoelasticity of poly(l-lactic acid), J. Polym. Sci. B Polym. Phys., 37 (1999), 1803-1814.
41. J.M. Ugartemendia, M.E. Muñoz, J.R. Sarasua, A. Santamaria, Phase behavior and effects of microstructure on viscoelastic properties of a series of polylactides and polylactide/poly(e-caprpolactone) copolymers, Rheologica Acta, 53 (2014), 857-868.
42. A. Sangroniz, L. Sangroniz, A. Gonzalez, A. Santamaria, J. Del Río, M. Iriarte, A. Etxeberria, Improving the barrier properties of a biodegradable polyester for packaging applications, Eur. Polym. J., 115 (2019), 76-85.
43. M.A. Corres, A. Mayor, A. Sangroniz, J. del Río, M. Iriarte, A. Etxeberria, Blends based on biodegradable poly(caprolactone) with outstanding barrier properties for packaging applications: the role of free volume and interactions, submitted.
44. A. Chaos, A. Sangroniz, A. Gonzalez, M. Iriarte, J. R. Sarasua, J. del Río, A. Etxeberria.Tributyl citrate as an effective plasticizer for biodegradable

polymers: effect of the plasticizer on the free volume, transport and mechanical properties, Polym. Int., 68 (2019), 125-133.

45. E.A. Mcgonigle, J.M.G. Cowie, V. Arrighi, R.A. Pethrick Enthalpy relaxation and free volume changes in aged styrene copolymers containing a hydrogen bonding co-monomer, J. Mater. Sci., 40 (2005), 1869-1881.
46. O. Miguel, J.J. Iruin, M.J. Fernandez-Berridi, Survey on transport properties of liquids, vapors, and gases in biodegradable poly(3-hydroxybutyrate) (PHB), J. Appl. Polym. Sci., 64 (1997), 1849–1859.
47. O. Miguel, J.J. Iruin, Evaluation of the transport properties of Poly(3-hydroxybutyrate) and its 3-hydroxyvalerate copolymers for packaging applications, Macromol. Symp., 144 (1999), 427–438.